Finite-Difference Time Domain Analysis of 1D Resonator

Sibi Chakravarthy Shanmugavel

ECE 5106 - Electromagnetic waves

The Finite Difference Time Domain method is a popular technique for the solution of electromagnetic problems. The simplicity of this method enables it to be applied to a wide variety of problems such as scattering from metal objects , antennas, microstrip circuits and many more. In this project, the method has been applied to perform a simulation of one of the simplest EM structures, i.e., free space bound by two planar perfect electric conductor (PEC) plates. This is a one-dimensional problem. In other words, the EM fields depend only on a single spatial variable (i.e., z). The 1D structure is simulated and a Fourier analysis is performed to determine the resonant frequencies of this structure

1 Introduction

The theory of FDTD method is based on discretizing, both in time and space, the Maxwell's equations with central difference approximations. The two Perfectly Electric Conductor plates are separated by free space. In this case, Maxwell's equations can be written as

$$\frac{\partial \vec{E}}{\partial t} = \frac{1}{\epsilon_0} \nabla \times \vec{H} \tag{1}$$

$$\frac{\partial \vec{H}}{\partial t} = \frac{-1}{\mu_0} \nabla \times \vec{E} \tag{2}$$

For a $\vec{z}$-directed, $\vec{x}$-polarized TEM wave ($H_z = E_z = 0$), incident upon a modeled geometry with no variations in the $\vec{x}$ and $\vec{y}$ direction, i.e. $\frac{\partial}{\partial x} = 0$ and $\frac{\partial}{\partial y} = 0$; equations (1) and (2) are reduced down to the 1D case:

$$\frac{\partial E_x}{\partial t} = \frac{-1}{\epsilon_o} \frac{\partial H_y}{\partial z} \tag{3}$$

$$\frac{\partial H_y}{\partial t} = \frac{-1}{\mu_o} \frac{\partial E_x}{\partial z} \tag{4}$$

Combining the partial space derivatives of (3) with the partial time derivative of (4) or vice versa produces the 1D scalar wave equation:

$$\left[\frac{\partial^2}{\partial z^2} - \epsilon\mu\frac{\partial^2}{\partial t^2}\right]\psi = 0 \tag{5}$$

where ψ represents either E_x or H_y. In the case of free-space where $\epsilon = \epsilon_0$ and $\mu = \mu_0$, equation (5) takes on the form:

$$\left[\frac{\partial^2}{\partial z^2} - \frac{1}{c^2}\frac{\partial^2}{\partial t^2}\right]\psi = 0 \tag{6}$$

where $c = \frac{1}{\sqrt{\mu_0\epsilon_0}}$ is the speed of light in vaccum.

2 Yee's FDTD algorithm

The 1D scalar wave equation can be solved directly using the centered second order differences. But, it is not efficient for solutions of problems that depend on both $\vec{E}$ and $\vec{H}$. In 1966, Kane Yee proposed an algorithm where the first order electric (3) and magnetic (4) equations are coupled via interlinked time and space grids. Because the underlying implementation of the Yee algorithm mimics the principle of a time varying electric field producing a time varying magnetic field and vice versa, solutions of more general class of problems can be handled robustly.

Yee's scheme consists in considering E_x and H_y shifted in space by half a cell and in time by half a time step when considering a central difference approximation of the derivatives. In such a case, equations (3) and (4) can be written as

$$\frac{E_x^{n+1/2}(k) - E_x^{n-1/2}(k)}{\Delta t} = -\frac{1}{\epsilon_o}\frac{H_y^n(k+1/2) - H_y^n(k-1/2)}{\Delta z} \tag{7}$$

$$\frac{H_y^{n+1}(k+1/2) - H_y^{n-1}(k+1/2)}{\Delta t} = -\frac{1}{\mu_o}\frac{E_x^{n+1/2}(k+1) - E_x^{n+1/2}(k)}{\Delta z} \tag{8}$$

Equations (7) and (8) show the usefulness of Yee's scheme in order to have a central difference approximation for the derivatives. In particular, the left term in equation (7) says that the derivative of the E field at time $n\Delta t$ can be expressed as a central difference using E field values at times $(n+1/2)\Delta t$ and $(n-1/2)\Delta t$. The right term in equations (7) approximates instead the derivative of the H field at point $k\Delta z$ as a central difference using H field values at points $(k+1/2)\Delta z$ and $(k-1/2)\Delta z$. This approximations oblige us to calculate always the E field values at points $\ldots$, $(k-1)\Delta z$, $(k)\Delta z$, $(k+1)\Delta z$, $\ldots$ and times $\ldots$, $(n-3/2)\Delta t$, $(n-1/2)\Delta t$, $(n+1/2)\Delta t$, $\ldots$ and to calculate always the H field values at points $\ldots$, $(k-3/2)\Delta x$, $(k-1/2)\Delta x$, $(k+1/2)\Delta x$, $\ldots$ and times $\ldots$, $(n-1)\Delta t$, $(n)\Delta t$, $(n+1)\Delta t$, $\ldots$

This way of staggering Electric field and magnetic field in time and space is known as the "leap-frog" algorithm. It provides us a means to approximate Maxwell's equations in space and time. The

H field values are updated first and then all E field values, remembering that E and H are shifted in space by half of the discretization Δz. This algorithm is depicted schematically in Figure 1

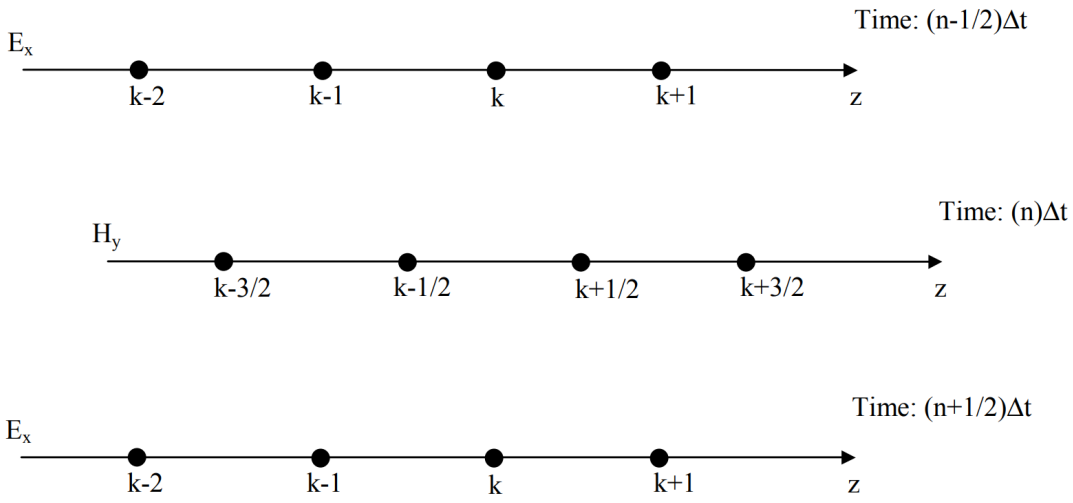

Figure 1: Yee's one-dimensional scheme for updating EM fields in space and time.

The explicit FDTD equations can be derived from (7) and (8) to give us,

$$E_x^{n+1/2}(k) = E_x^{n-1/2}(k) - \frac{\Delta t}{\epsilon_o \Delta z}[H_y^n(k+1/2) - H_y^n(k-1/2)] \tag{9}$$

$$H_y^{n+1}(k+1/2) = H_y^n(k+1/2) - \frac{\Delta t}{\mu_o \Delta z}[E_x^{n+1/2}(k) - E_x^{n+1/2}(k+1)] \tag{10}$$

The above equations can be directly implemented using a programming language. It should be noted that the "1/2" in equations (9) and (10) are just a physical definition of Electric and Magnetic field i.e. they only represent the fact that E and H are actually offset by half a cell and half a time step. But, this notation will not appear in the coding because programming language data arrays support only integer array indices. The algorithm to implement the code for the calculation of the Electric and Magnetic fields obeying to equations (9) and (10) is as follows,

1. The cell size Δz is chosen and the corresponding size of the arrays E and H are determined. The array size,N, is the number of FDTD cells used for the computation.The absolute size of the computational domain is given by $N \times \Delta z$

2. Once the cell size has been chosen, the time step size necessary for the computation is determined according to the resolution needed. The time step is chosen according to stability considerations. For stability reasons, a field component cannot propagate more than one cell size in the time step Δt. This means that

$$\Delta t \leq \frac{\Delta z}{c_o} \tag{11}$$

since the wave travels at the speed of the light c_o. This is the stability condition for one-dimensional problems.

3. The total number of time steps is chosen and a cycle is implemented to compute the fields for each time step. Within the cycle,

   - A cycle is implemented to calculate the $E_x(k)$ values according to equation (9) for all the cells of the computational domain
   - The excitation signal at the source point for each time step is computed.
   - A cycle is implemented to calculate the $H_y(k)$ values according to equation (10) for all the cells of the computational domain

3 One Dimensional Cavity Resonator

3.1 Problem statement and setup

The problem statement corresponds to the simulation of an one dimensional rectangular cavity i.e., free space bound by two planar perfect electric conductor (PEC) plates. In this case,the EM fields depend only on a single spatial variable (i.e., z). The PEC plates extend infinitely in the X and Y directions.

The distance between the two PEC plates is L=30. The size of the field array i.e. the number of FDTD cells is chosen to be 31 where the cells k=1 and k=31 are chosen to be the PEC plate boundaries.

3.2 Boundary conditions

Since the boundaries are given by a perfect electric conductor, we apply the corresponding boundary conditions. At the boundary of an electric conductor, the tangential electric field and the normal magnetic field are zero. Also, inside a PEC material, no fields can exist.

In the cell n=1, we set the tangential electric field $E_x = 0$,but $H_y \neq 0$. In cell k=31, we set both E_x and H_y to zero because the cell k=31 is entirely made up of PEC material.

3.3 Source signal

For this simulation, the source signal is chosen to be a Gaussian pulse and the source point is the k=16 cell. A Gaussian signal centred at t_o given by

$$g(t) = exp^{-\frac{1}{2}(\frac{t-t_o}{\sigma})^2} \tag{12}$$

is used as the source signal

3.4 Matlab implementation

A matlab code has been written according to the algorithm described in section 2. The correspondence between physical and computer variables is indicated in the following figure.

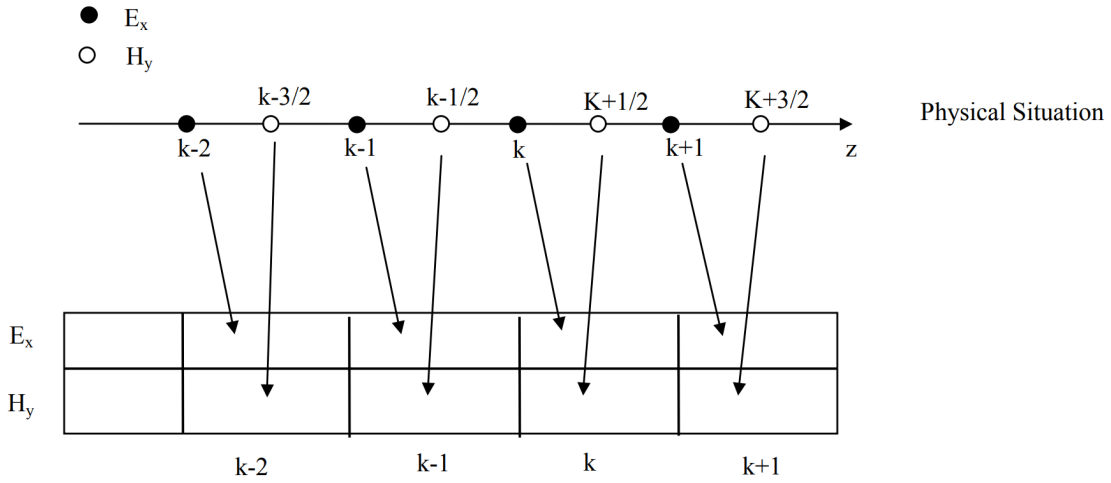

Figure 2: Relation between programmed array and the physical array.

The matlab code to implement the algorithm is given as follows,

```
N=31;
Sp=floor(N/2);
nsteps=10^4;
% Cell size and time stepping
c0=1;dz=1;dt=0.5;cc=c0*dt/dz;
ex=zeros(1,N);
hy=zeros(1,N);
t0=20;
spread=6;
M=moviein(nsteps);
for t=1:nsteps
ex(1)=0;
ex(ke)=0;
for k=2:ke-1
ex(k)=ex(k)+cc*(hy(k-1)-hy(k));
end
    ex(ks)=ex(ks)+exp(-.5*((t-t0)/spread)^2);
for k=1:ke-1
hy(k)=hy(k)+cc*(ex(k)-ex(k+1));
end
plot(ex);axis([1 ke -2 2]);
```

```
M(:,t) = getframe ;
E(t)=ex(6);
H(t)=hy(6);
end
movie(M,1);
figure
Fs=1/dt;
n = 2^nextpow2(numel(E));
Y = fft(E,n);
f = Fs*(0:(n/2))/n;
P = abs(Y/n);
plot(f,P(1:n/2+1))
figure
Y = fft(H,n);
f = Fs*(0:(n/2))/n;
P = abs(Y/n);
plot(f,P(1:n/2+1))
```

4 Computer simulation

Having described the formulations and basic pseudo code implementations of various parts of the one-dimensional FDTD algorithm, the simulation results are discussed and analysed in this section.

4.1 Initialization

Initialization is performed at the beginning of the simulation. Fig. 3 shows the initialized 1D space grid of $E_x(k)$ and $H_y(k)$ at time t = 0.

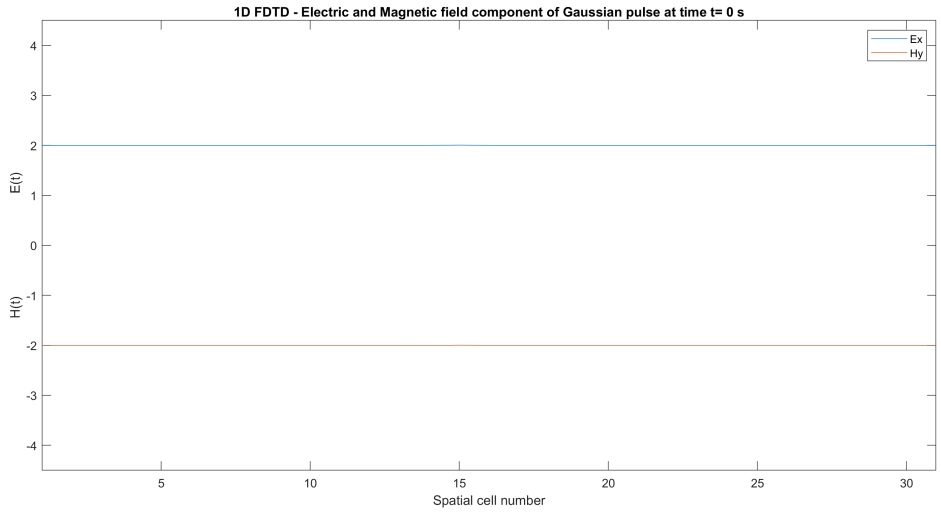

Figure 3: Space grid initialization at time t = 0s.

4.2 Simulation Output

In this section, the PEC boundary condition at z=0 and z=31 is enforced. The Gaussian pulse is closely followed in space and its spatial cell values are recorded at every time step. Figures (4-13) shows the variation of $E_x(k)$ and $H_y(k)$ at different times.

From basic electromagnetic theory, it is expected that the tangential electric field to be zero on the PEC; Therefore, the reflected electric field must be 180 degrees out of phase compared to that of the incident field. This result is shown in Fig. 6 and Fig. 7 by comparing the incident $E_x(k)$ before colliding with the PEC to the reflected $E_x(k)$ after colliding with the PEC.

During the collision, part of the incident pulse reflects off the PEC and interferes with its own trailing tail; this interference happens to be constructive in E_x but destructive in H_y due to the phase difference of pi between them. This can be observed in Fig. 10

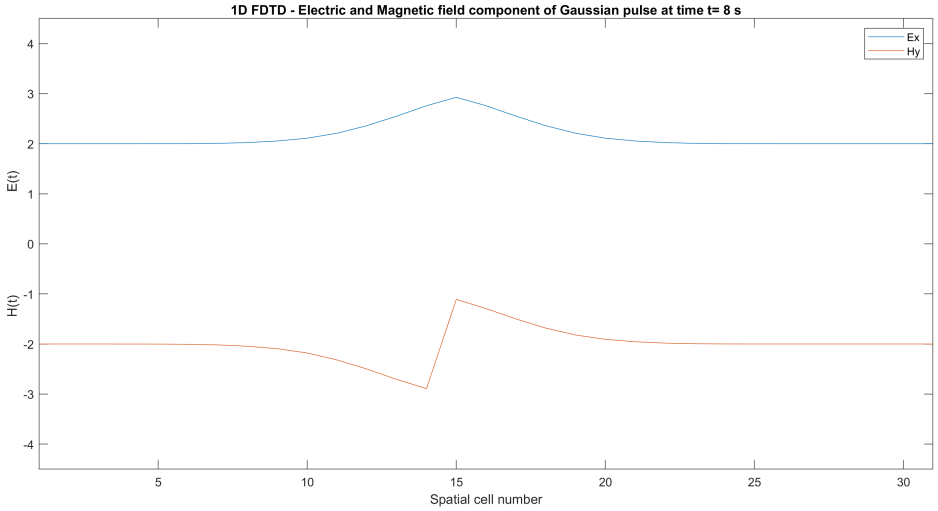

Figure 4: Pulse propagation at t=8s.

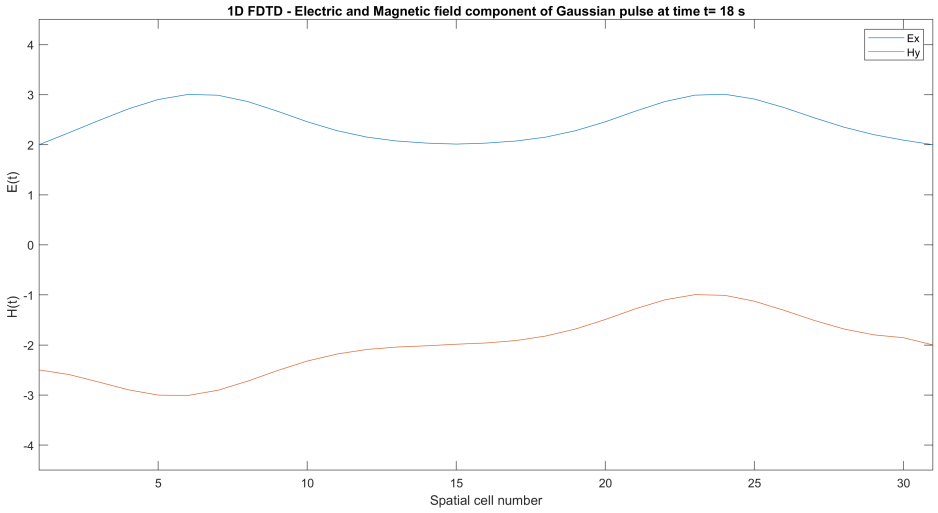

Figure 5: Pulse propagation at t=18s.

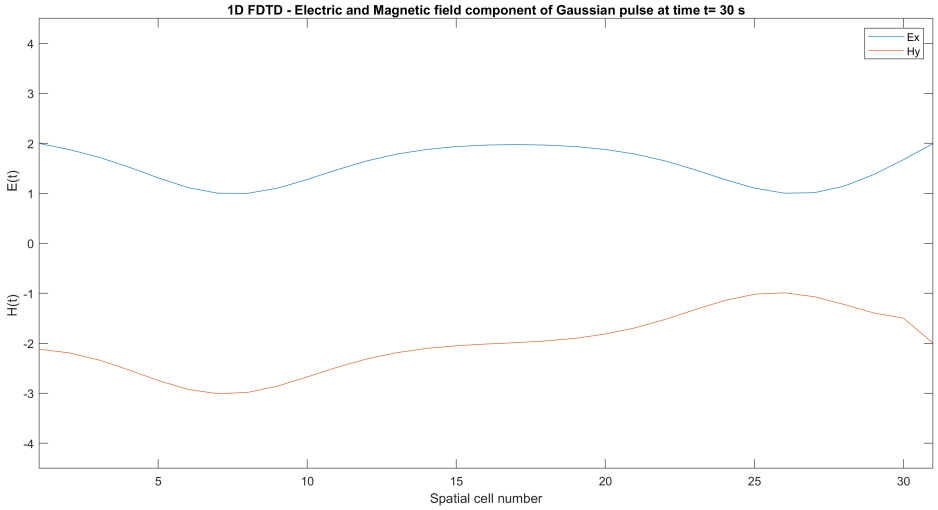

Figure 6: Pulse propagation at t=30s.

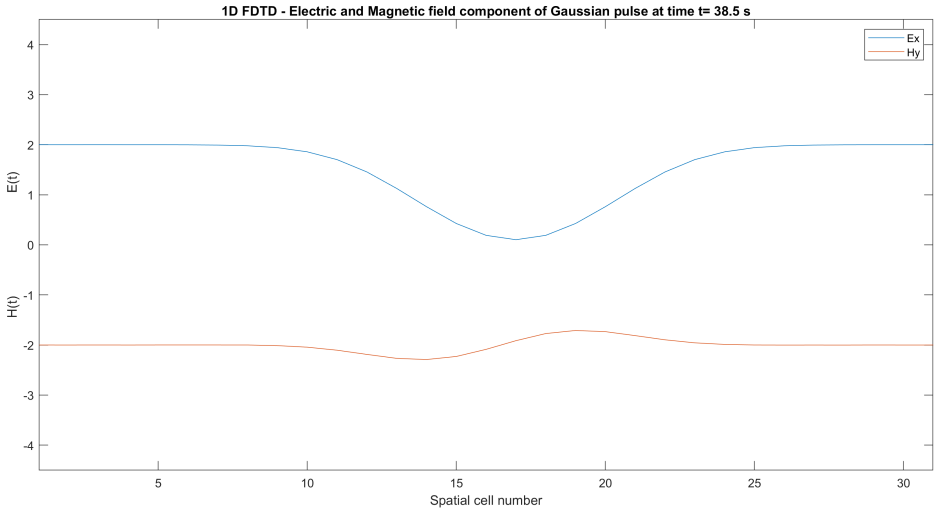

Figure 7: Pulse propagation at t=38.5s.

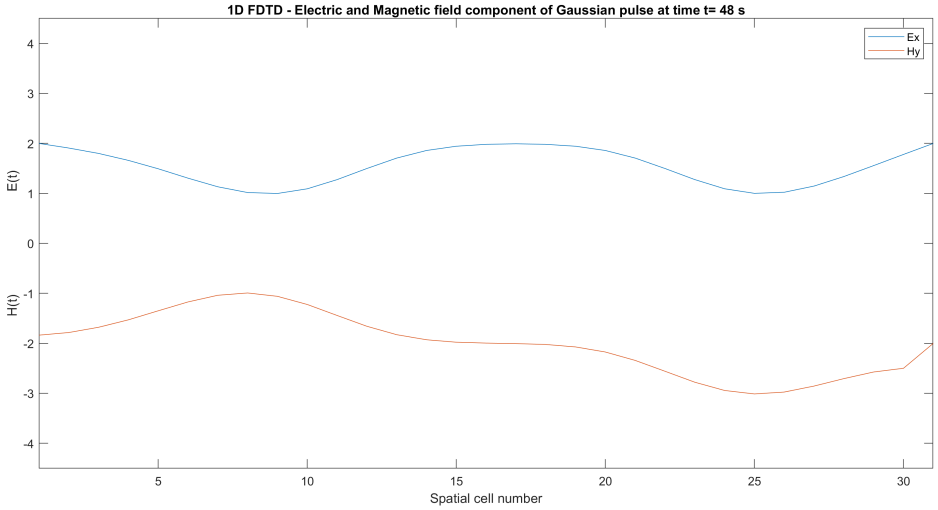

Figure 8: Pulse propagation at t=48s.

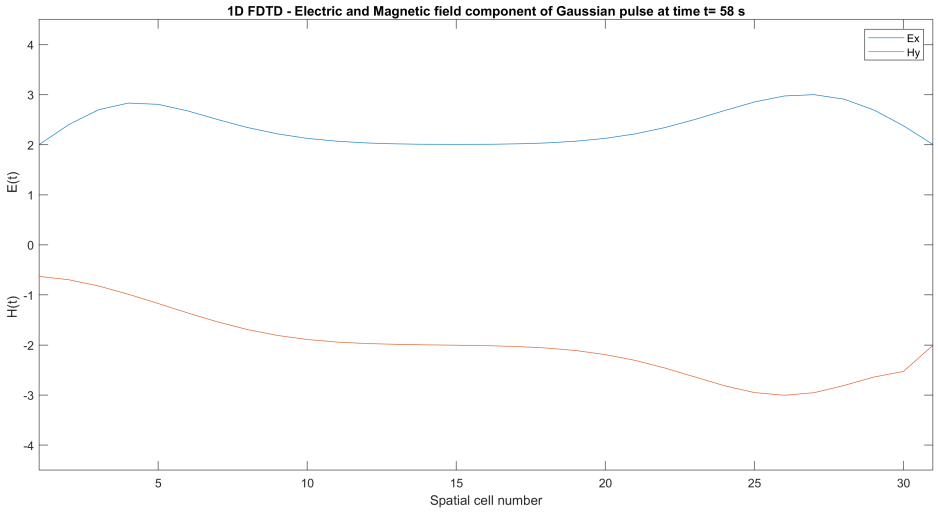

Figure 9: Pulse propagation at t=58s.

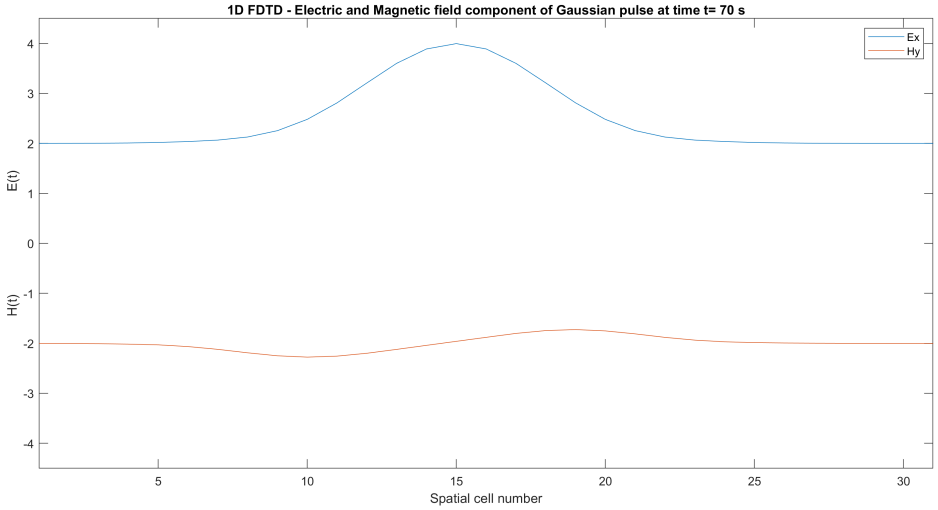

Figure 10: Pulse propagation at t=70s.

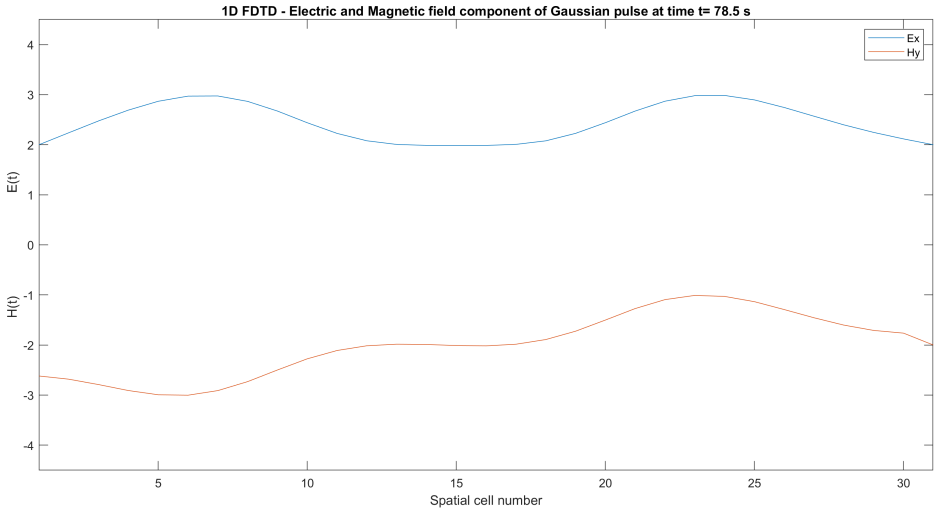

Figure 11: Pulse propagation at t=78.5s.

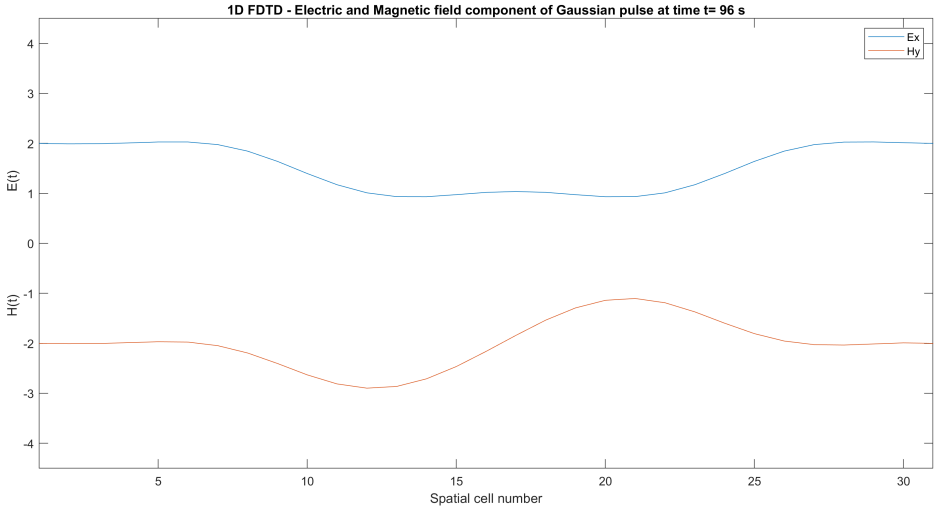

Figure 12: Pulse propagation at t=96s.

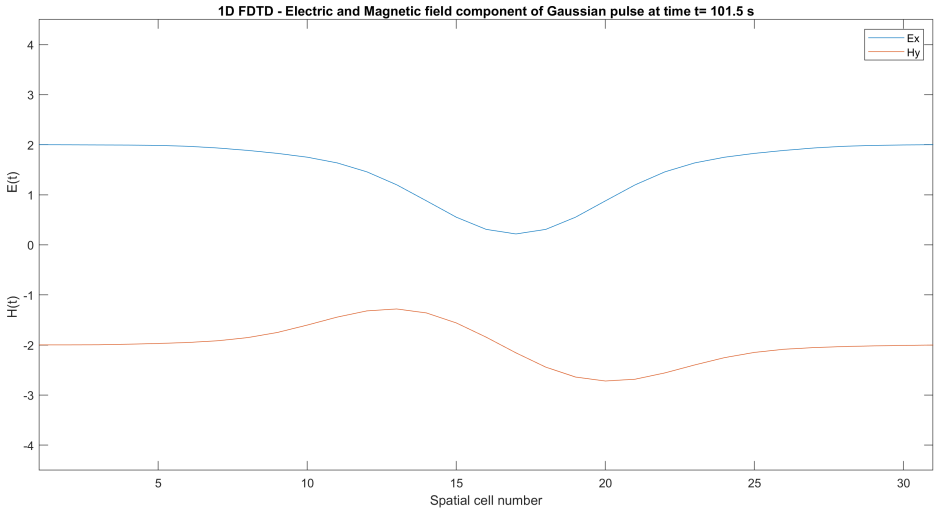

Figure 13: Pulse propagation at t=101.5s.

5 Fourier Analysis

In this section, a Fourier transform of the Electric and Magnetic fields is performed and they are obtained as a function of frequency

The electric and magnetic field values at the 6^{th} cell are recorded at all time instants and a Fourier analysis is performed on these field values to convert from time domain to frequency domain to determine the resonant frequencies of the 1D resonant cavity.

Firstly the dimension of the resonant cavity is determined using the formula $d = \Delta z \times N$

where N is the number of cells separating the two PEC plates and Δz is the spacing between each cell.

Here, we have N=31 cells and each cell separated by 1 unit. The structure is modelled such that the 1^{st} cell is a PEC boundary and the 31^{st} cell is entirely made up of PEC. Hence, the two PEC plates are separated by 30 cells. Thus, $d = \Delta z \times N = 30 \times 1 = 30$

The resonant frequency modes for a 3D cavity resonator is given by,

$$f_{m,n,l} = \frac{c}{2\sqrt{\mu_r \epsilon_r}} \sqrt{\left(\frac{m}{a}\right)^2 + \left(\frac{n}{b}\right)^2 + \left(\frac{l}{d}\right)^2} \tag{13}$$

Where a, b and d are the dimensions of the cavity along the x, y and z directions. μ_r and ϵ_r are the relative permeability and relative permittivity of the material inside the resonant cavity respectively. 'c' is the speed of light; m, n, and l are the mode numbers.

In the given 1D cavity, wave propagates only along the z direction which means there is a standing wave pattern only along the z direction. The PEC plates extend infinitely along the x and y directions. By substituting a and b as infinity in the above equation, we determine the resonant frequency formula for a 1D cavity resonator.

$$f_l = \frac{c}{2\sqrt{\mu_r \epsilon_r}} \left(\frac{l}{d}\right) \tag{14}$$

In our case we have free space bounded by two PEC plates. Hence, $\mu_r = 1$ and $\epsilon_r = 1$. Also, we normalize our units such that $\mu_0 = 1$ and $\epsilon_0 = 1$ to give c=1. The final equation for determining resonant frequencies is given by,

$$f_l = \frac{1}{2} \left(\frac{l}{d}\right) \tag{15}$$

5.1 Theoretical calculation

The theoretical values of the resonant frequencies are determined using equation (15) for each particular mode number for the 1D cavity under consideration.

For l=1, $f_1 = \frac{1}{2}\left(\frac{1}{30}\right) = 0.0166\ Hz$

For l=2, $f_2 = \frac{1}{2}\left(\frac{2}{30}\right) = 0.0333\ Hz$

For l=3, $f_3 = \frac{1}{2}\left(\frac{3}{30}\right) = 0.05\ Hz$

For l=4, $f_4 = \frac{1}{2}\left(\frac{4}{30}\right) = 0.066\ Hz$

For l=5, $f_5 = \frac{1}{2}\left(\frac{5}{30}\right) = 0.0833\ Hz$

In a similar way, the higher order resonant mode frequencies are computed using (15).

5.2 Matlab verification

The matlab program is used to verify the theoretical resonant frequencies. The electric field and magnetic field values at the 6^{th} cell are recorded for all time steps. A Fourier transform of this time sequence values is computed to determine the frequency spectrum.

The resonant frequencies for each EM mode determined from the Fourier analysis are as follows,

For l=1, $f_1 = 0.0166\ Hz$

For l=2, $f_2 = 0.0333\ Hz$

For l=3, $f_3 = 0.0498\ Hz$

For l=4, $f_4 = 0.06628\ Hz$

For l=5, $f_5 = 0.08264\ Hz$

The frequency spectrum of the EM field is shown in Figures (14), (15), (16) and (17)

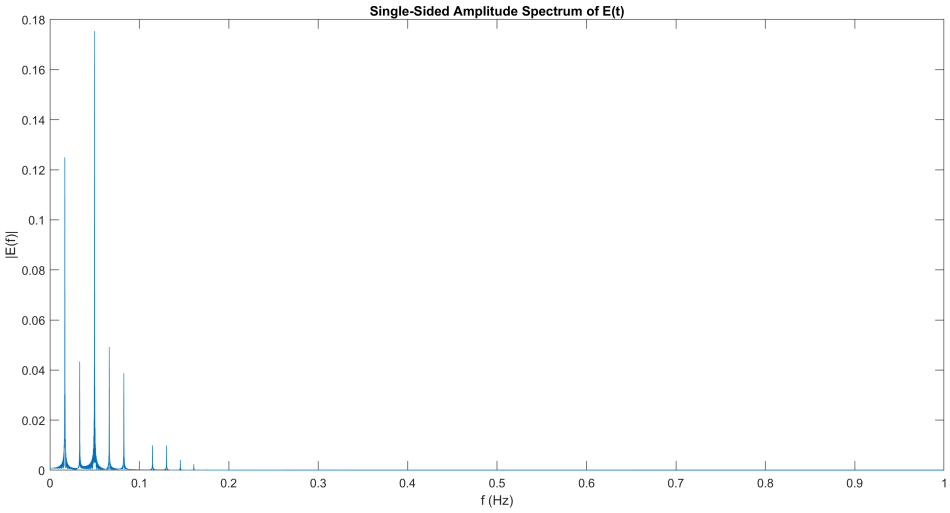

Figure 14: Frequency spectrum of Electric field $E_x(t)$.

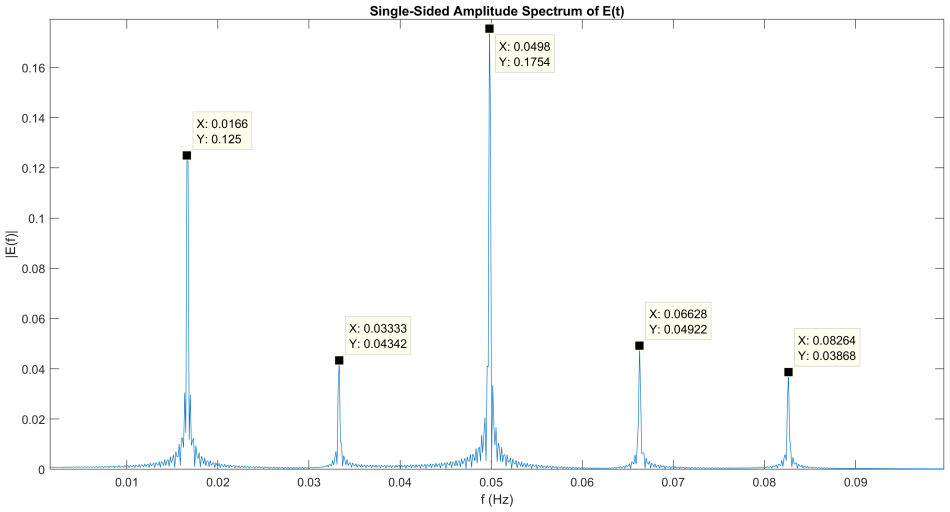

Figure 15: Magnified frequency spectrum of Electric field $E_x(t)$.

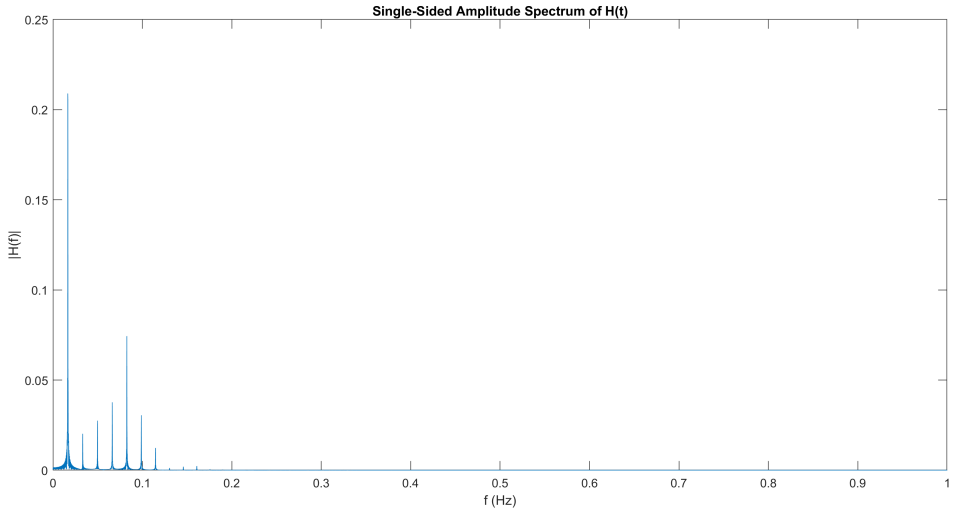

Figure 16: Frequency spectrum of Magnetic field $H_y(t)$.

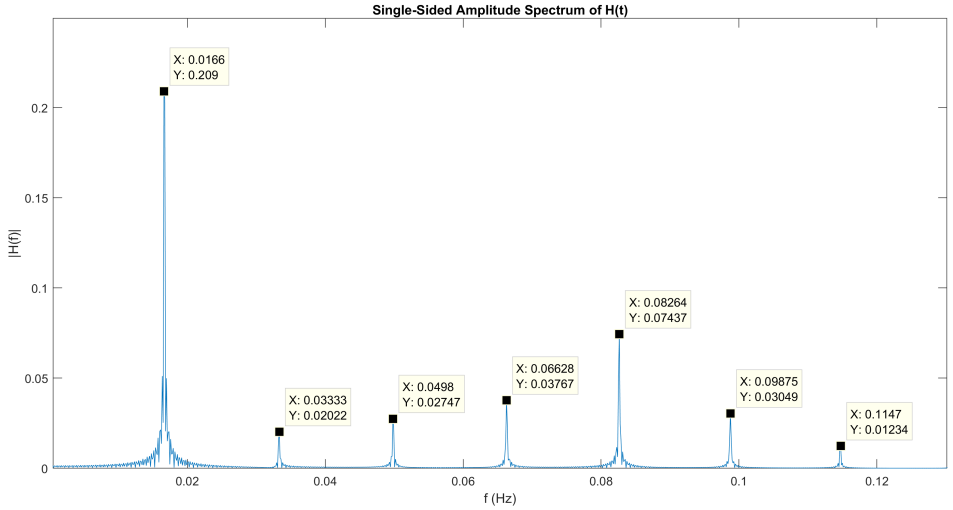

Figure 17: Magnified frequency spectrum of Magnetic field $H_y(t)$.

The values of the resonant frequencies determined through Fourier analysis are found to match exactly with the theoretical values computed using equation (15). This proves the validity of the algorithm.

6 Spatial Dependence of resonant modes

In this section, the spatial dependence of the EM modes supported by this 1D structure is extracted.

To determine the spatial dependency of a resonant mode, the EM field value at each individual cell for all time steps are recorded. A Fourier transform of the time varying EM field value for each spatial cell is performed separately to obtain them as a function of frequency.

A Finite impulse response(FIR) band pass filter has been designed to filter the resonant frequency corresponding to a specific EM mode. The input signal from each spatial cell is convolved with the filter response to get the corresponding filtered output signal. The output signal will have only a single frequency component corresponding to the specific EM mode for which the filter was designed.

We can predict the spatial dependency of an EM mode by using the fact that the mode number corresponds to the number of half wavelengths within the structure. For instance, l=1 mode can be expected to have one half wavelength; l=3 mode can be expected to have three half wavelengths ; l=5 mode can be expected to have five half wavelengths and so on.

The process is illustrated for three different modes below,

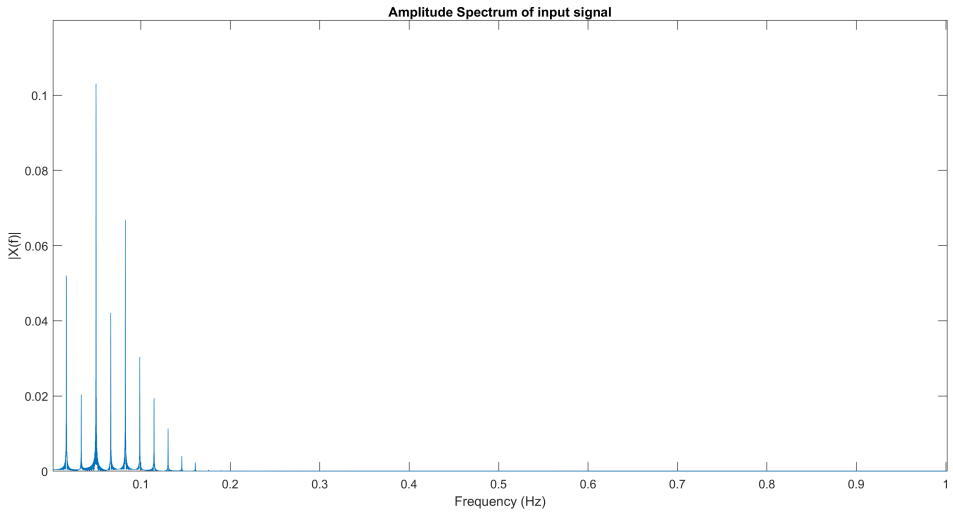

Figure 18: Frequency spectrum of Electric field E(t) for cell k=2.

Spatial dependency of l=3 Mode

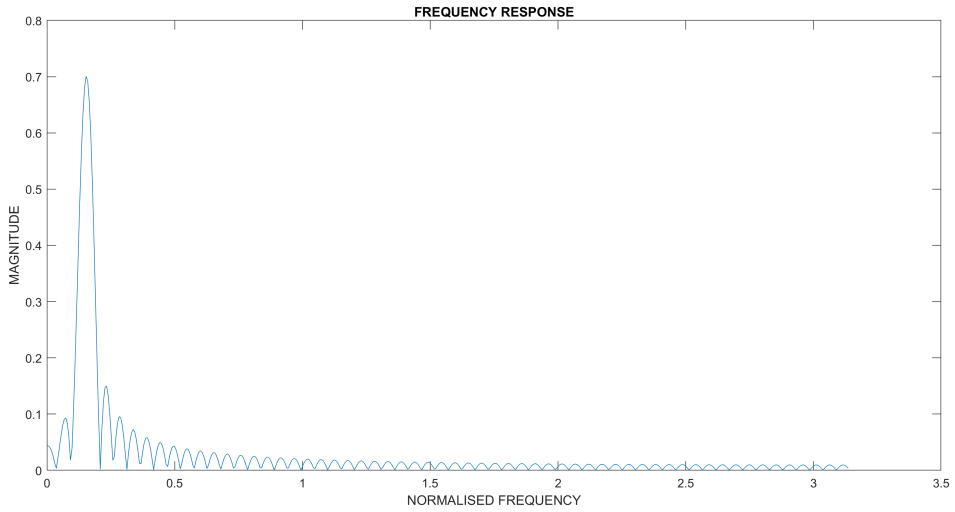

Figure 19: Frequency response of FIR band pass filter for l=3 mode.

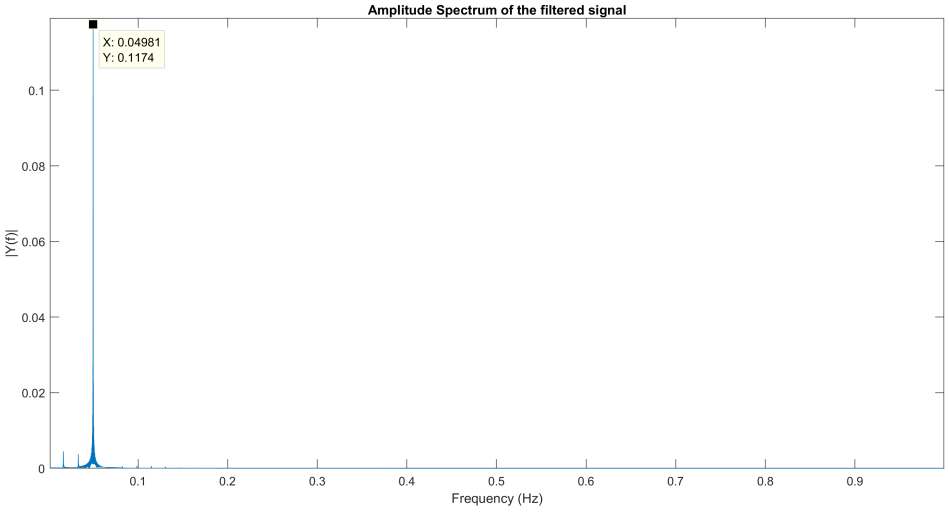

Figure 20: Frequency spectrum of filtered Electric field E(t).

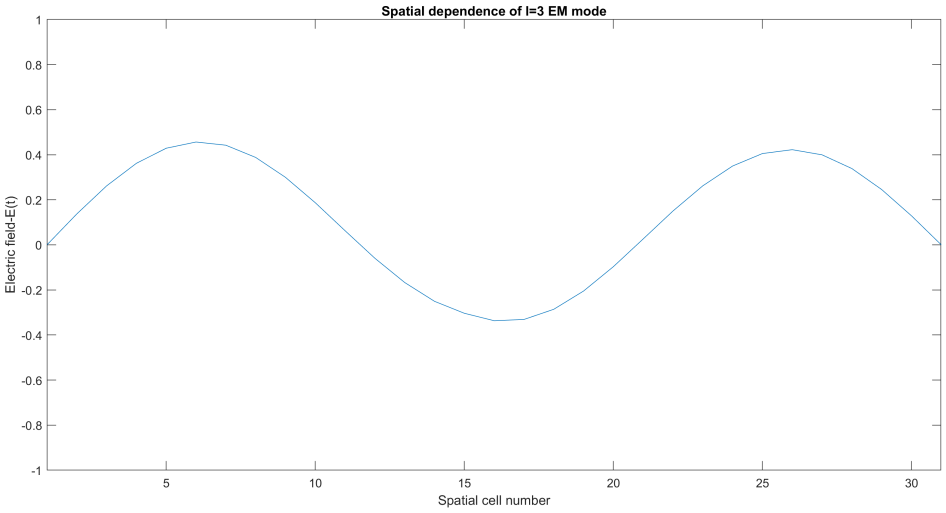

Figure 21: Spatial dependence of l=3 mode.

It is clearly observed that the l=3 resonant EM mode has three half wavelengths making our prediction valid.

Spatial dependence of l=5 Mode

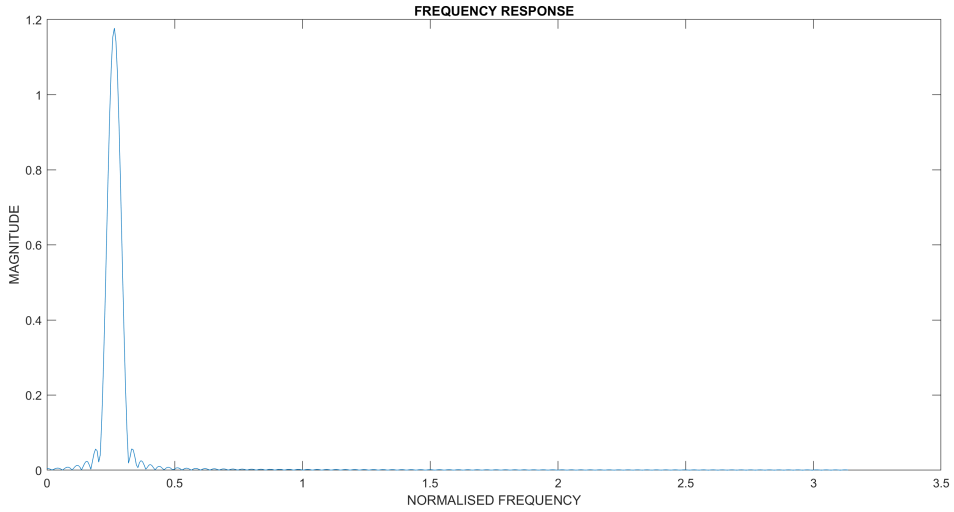

Figure 22: Frequency response of FIR band pass filter for l=5 mode.

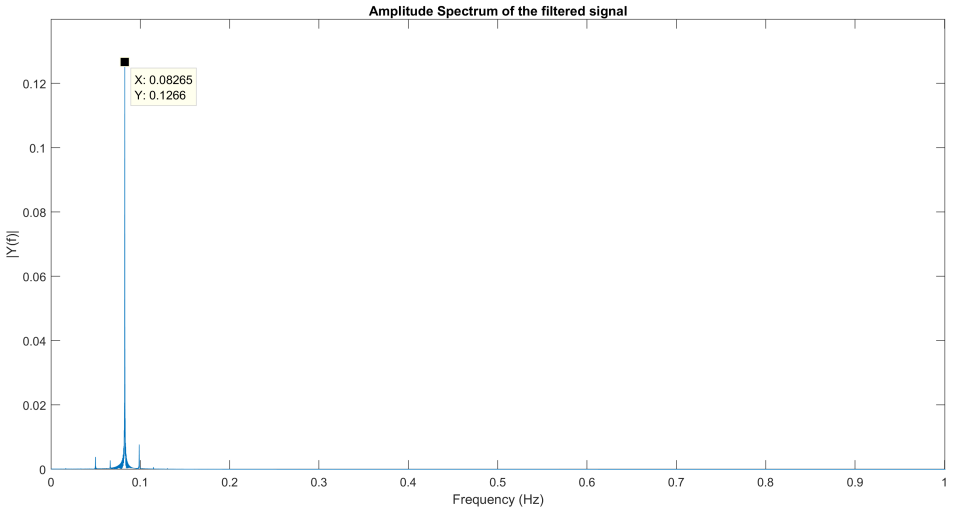

Figure 23: Frequency spectrum of filtered Electric field E(t).

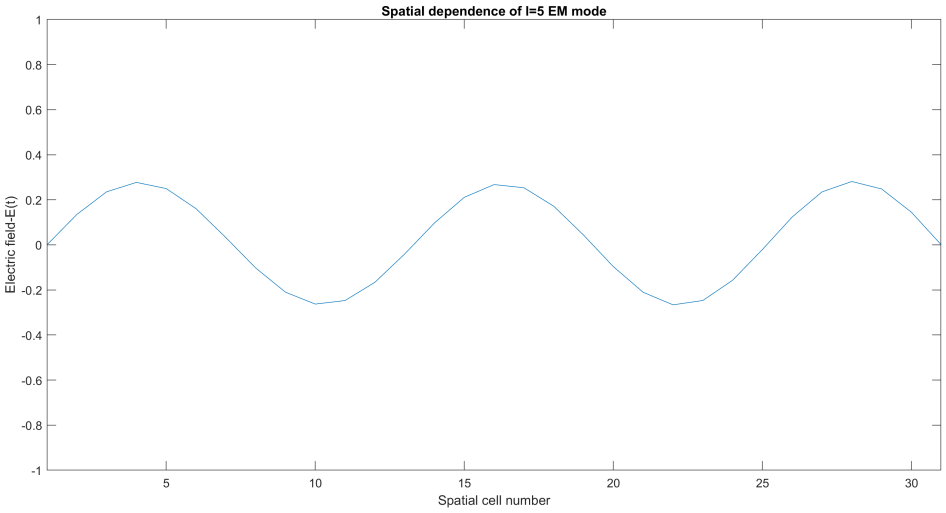

Figure 24: Spatial dependence of l=5 mode.

As expected, the l=5 resonant cavity mode has five half wavelengths matching exactly with the theoretical prediction.

Spatial dependence of l=1 Mode

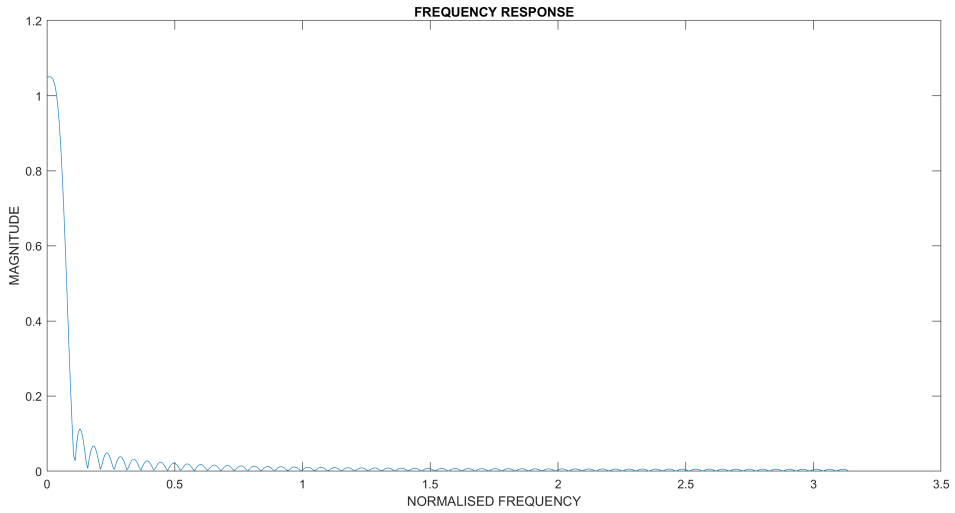

Figure 25: Frequency response of FIR band pass filter for l=1 mode.

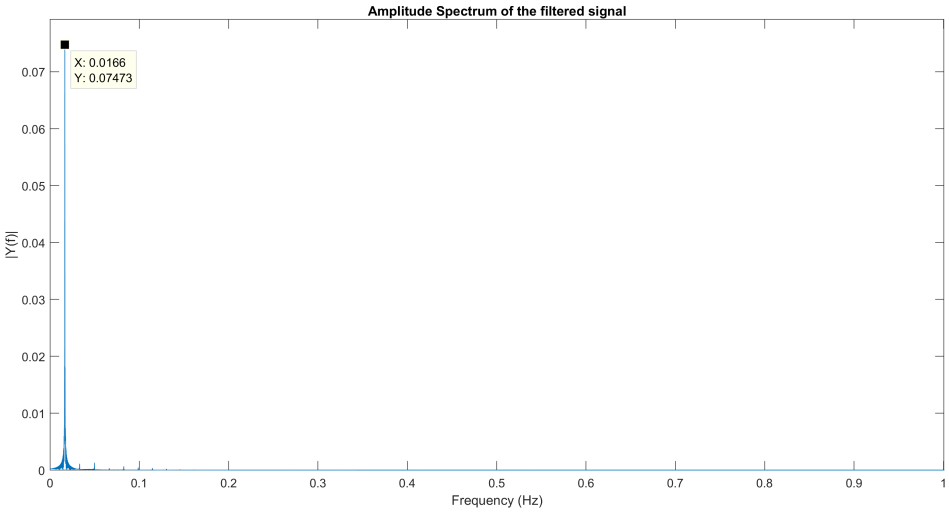

Figure 26: Frequency spectrum of filtered Electric field E(t).

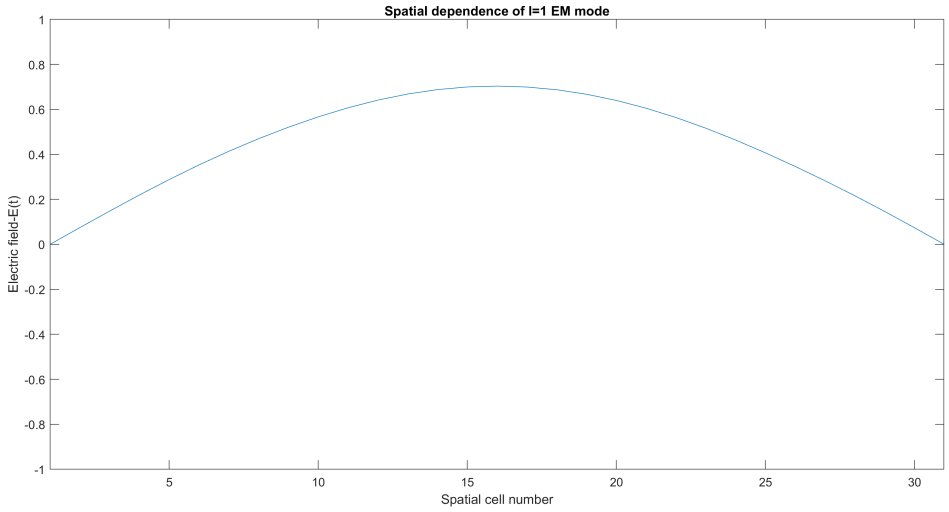

Figure 27: Spatial dependence of l=1 mode.

Again, as expected the l=1 resonant cavity mode has one half wavelength matching exactly with the theoretical prediction.

The same process can be repeated to extract the spatial dependency of any resonant mode supported by this 1D structure. The only change will be the upper cut off and lower cutoff frequency for the FIR band pass filter for each specific mode.

6.1 Code

```
fprintf('\nFIR BAND PASS FILTER\n');
N=170;%input('ENTER THE ORDER  ');
WL=0.0725*pi; %Lower cutoff frequency
WU=0.095*pi; %Upper cutoff frequency
m=(N-1)/2;
h=zeros(1,N);
hd=zeros(1,N);
for n=0:N-1
    hd(n+1)=(sin((n-m)*WU)-sin((n-m)*WL))./((n-m)*pi);
    if n==m
        hd(n+1)=(2*WU-2*WL)/(2*pi);
    end
    h(n+1)=hd(n+1);
end
[FRF,WF]=freqz(h,1);
Fs =1/0.5;
T = 1/Fs;
figure
set(gca, 'FontSize', 16)
plot(WF,(abs(FRF)));
title('FREQUENCY RESPONSE');
xlabel('NORMALISED FREQUENCY');
ylabel('MAGNITUDE');
%APPLICATION
E=E3;
L = numel(E);
inputsig= E;
NFFT = 2^nextpow2(L); Next power of 2 from length of y
Y = fft(inputsig,NFFT);
% Y=Y.*conj(Y);
%f = Fs/2*linspace(0,1,NFFT/2+1);
f = Fs*linspace(0,1,NFFT);
figure
set(gca, 'FontSize', 16)
plot(f,abs(Y(1:NFFT)/NFFT))
title('Amplitude Spectrum of input signal');
xlabel('Frequency (Hz)');
ylabel('|X(f)|');
%PSD OF FILTERED SIGNAL
y=filter(h,1,inputsig);
NFFT = 2^nextpow2(L);%Next power of 2 from length of y
Y = fft(y,NFFT)/L;
f = Fs*linspace(0,1,NFFT);
% Plot single-sided amplitude spectrum.
figure
set(gca, 'FontSize', 16)
```

```
plot(f,abs(Y(1:NFFT)))
title('Amplitude Spectrum of the filtered signal')
xlabel('Frequency (Hz)')
ylabel('|Y(f)|')
```

7 Conclusion

This report successfully demonstrates a working 1D-FDTD code that correctly implements a PEC boundary to investigate an one dimensional cavity resonator. Through Matlab simulation and a Fourier analysis, it was found that the theoretical resonant frequencies match exactly with the values determined using Fourier analysis. In addition, a FIR band pass filter has been designed to extract the spatial dependence of a specific EM mode supported by this 1D structure.